論文 / 著書情報
Article / Book Information

Title	Band offsets of CuInSe2/CdS and CuInSe2/ZnS (110) interfaces: A hybrid density functional theory study
Authors	Yoyo Hinuma, Fumiyasu Oba, Yu Kumagai, Isao Tanaka
Citation	Physical Review B, vol. 88, , pp. 035305
Pub. date	2013, 7
Copyright	(c) 2013 American Physical Society
DOI	http://dx.doi.org/10.1103/PhysRevB.88.035305

Band offsets of $CuInSe_2$/CdS and $CuInSe_2$/ZnS (110) interfaces: A hybrid density functional theory study

Yoyo Hinuma,[1,*] Fumiyasu Oba,[1,2,†] Yu Kumagai,[2] and Isao Tanaka[1,3]
[1]*Department of Materials Science and Engineering, Kyoto University, Kyoto 606-8501, Japan*
[2]*Materials Research Center for Element Strategy, Tokyo Institute of Technology, Yokohama 226-8503, Japan*
[3]*Nanostructures Research Laboratory, Japan Fine Ceramics Center, Nagoya 456-8587, Japan*
(Received 19 April 2013; published 11 July 2013)

The valence band offsets of the $CuInSe_2$/CdS and $CuInSe_2$/ZnS (110) interfaces are obtained based on various definitions using first-principles calculations in the framework of hybrid density functional theory. Both the strained band offset and the unstrained, or natural, band offset are investigated, where the two phases share and do not share in-plane lattice parameters perpendicular to the stacking direction, respectively. The valence band offset is determined by first obtaining the difference between the reference levels of two phases in the regions far from the interface and then adding the difference between the valence band maximum and the reference levels of bulk for the two phases. The nonfaceted (110) interface and a number of (112)/(11$\bar{2}$) faceted interfaces, some containing ordered point defects in the $CuInSe_2$ (CIS) region, are considered. The excess energies of CIS/CdS and CIS/ZnS interfaces are lower when there are no ordered point defects, in contrast to the CIS surfaces that stabilize with ordered defect formation. The valence band offset is not significantly dependent on the atomic configurations at the interface as long as there are no charged layers. Surface calculations suggest that the reference level, which is determined by the average electrostatic potential at the atomic site, is not strongly dependent on lattice strain. A definition of the natural valence band offset that assumes a strain-invariant difference in the reference levels of the two phases provides values almost independent of the in-plane lattice parameters used in the interface calculation, which are about −1.2 and −1.3 eV with respect to CIS for the CIS/CdS and CIS/ZnS interfaces that contain no charged layers, respectively. The ionization potential difference can differ from the natural valence band offset by up to 0.3 eV without any consistent tendency to overestimate or underestimate, showing that the ionization potential difference is not necessarily a reasonable measure of the natural valence band offset.

DOI: 10.1103/PhysRevB.88.035305 PACS number(s): 73.20.Hb, 73.40.Lq, 68.35.bg

I. INTRODUCTION

The heterostructure of a $CuInSe_2$ (CIS) photoabsorber and a CdS layer is a prototypical system for $CuIn_{1-x}Ga_xSe_2$ (CIGS) thin-film solar cells.[1–6] Understanding of the properties of such model systems is essential because it provides the fundamentals for design and development of CIGS cells. In particular, the offsets of the valence and conduction bands at heterointerfaces are important quantities that affect the conversion efficiency.[7,8] A number of experimental studies have determined the band offsets at CIS/CdS interfaces, mostly for the valence band, using ultraviolet[2–4,6,9,10] and x-ray[2,4,6,11] photoelectron spectroscopy.

In general, the accurate determination of the valence and conduction band offsets at heterointerfaces is an important problem not only in solar cells but also in virtually all electronic and optoelectronic devices using semiconductor and/or insulator heterostructures. Therefore, this topic has been discussed for decades.[12] The band offset denotes the discontinuity in the band edges at the interface between two constituent semiconductors or insulators.[12,13] However, the band edges cannot be exactly defined within a few atomic layers near the interface because the electronic structure can be substantially altered there. Thus, an appropriate approach is to measure the band positions in a region sufficiently far from the interface in the absence of band bending associated with carrier redistribution.

The valence band offset at an interface can be estimated by using the ionization potential (IP) of surfaces because the valence band maximum (VBM) of any material can be aligned against the vacuum level by using the IP. Computationally, the IP is obtained using models composed of slabs separated by vacuum. There are many definitions of the IP; some definitions explicitly include the effects of surface localized states[14,15] while the "bulk-based" IP is defined as the difference between the vacuum level and the VBM in the bulklike region far from the surface.[15] Most definitions, including the bulk-based IP, are affected by the surface dipole in the thickness direction that is induced by the relaxation of the atomic positions and the electron charge distribution near the surface.

Direct calculations of interfaces are appealing because there are no artificial surface effects included in the offset evaluation. The problem here is that heterointerfaces in semicoherent structures with misfit dislocations or incoherent structures cannot be readily modeled in view of the variety and complication in the atomic structure as well as the high computational cost. In many cases, coherent interfaces, where in-plane lattice parameters (ILPs) are the same in the two constituent phases, are treated under three-dimensional periodic boundary conditions. This approach is appropriate to an actually coherent interface, such as the interface between a substrate and an epitaxial film of a second phase that is thinner than the critical thickness. However, some corrections need to be made regarding the ILPs to obtain the offset between unstrained constituent phases, which is called the "unstrained" or "natural" band offset, where the ILPs of the two phases are allowed to relax. One approach for evaluating the natural band offset uses a coherent interface calculation to obtain the difference between reference levels of two constituent semiconductors, which are given by the electrostatic potential

or core levels, and the absolute deformation potential[16–19] to correct the VBM of each semiconductor.[20–22] The relative shifts of the reference level as well as the VBM against an external standard need to be considered for accurate evaluation of the natural band offsets because both the reference level and the VBM shift independently with deformation. Lany *et al.*[23] used an alternative approach, where the average electrostatic potential at the atomic site was used as a reference to obtain the strained band offsets between NiO, ZnO, and MgO, and then IPs for strained and unstrained surfaces were used to remove the influence of strain to predict the natural band offsets. As mentioned above, many methods have been proposed to calculate the band offset, but we are not aware of any comprehensive study that evaluates, compares, and discusses the differences in the band offset of the same system obtained through various methods.

In this study, the stability and valence band offsets of the interfaces between the chalcopyrite CIS (110) and zincblende CdS or ZnS (110) are investigated using first-principles calculations based on hybrid density functional theory. Various methodologies using surface and/or coherent interface models are considered for the evaluation of the band offsets. Formation of (112) and (11$\bar{2}$) facets together with point defects has been suggested to stabilize the CIS (110) surface,[15,24,25] and therefore a number of interface configurations including nonfaceted and faceted structures with and without point defects are investigated.

II. METHODOLOGY

A. Computational procedures

The calculations were performed in the framework of the generalized Kohn-Sham scheme[26] using the projector-augmented wave (PAW) method[27] and the Heyd-Scuseria-Ernzerhof (HSE06) hybrid functional[28–30] as implemented in the Vienna *Ab initio* Simulation Package (VASP).[31–34] A plane-wave cutoff energy of 400 eV and PAW datasets with the following valence electronic states and radial cutoffs[33] were used: $3d$, $4s$, $4p$, and 1.2 Å for Cu; $5s$, $5p$, and 1.6 Å for In; $4d$, $5s$, $5p$, and 1.2 Å for Cd; $3d$, $4s$, $4p$, and 1.2 Å for Zn; $4s$, $4p$, and 1.1 Å for Se; and $3s$, $3p$, and 1.0 Å for S. The HSE06 hybrid functional has been applied to a variety of semiconductors and shown to describe their atomic and electronic structures much better than local and semilocal functionals.[30,34–39] The optimal amount of the Hartree-Fock exchange mixing in hybrid functionals is system dependent,[40,41] and the tuning of the mixing has been made to better describe the electronic structure of semiconductors.[40,42,43] In the present study, the Hartree-Fock exchange mixing in the HSE06 functional was set at $a = 0.30$ in addition to the standard value of $a = 0.25$, as the former reproduces the band gap of CIS better.[15,44]

Four types of structures were considered for each of CIS/CdS and CIS/ZnS (110) interfaces in this work. Previous first-principles studies using the local density approximation (LDA)[24] and HSE06 ($a = 0.30$)[15] show that the CIS (110) surface has low energy when there are (112) and (11$\bar{2}$) facets and a high concentration of ordered point defects. There are two sets of point defect orderings that result in low surface energy. In the first set, the Cu atoms on the cation-terminated surface become vacancies (V_{Cu}) and half of the Cu atoms on the anion-terminated surface become In antisites ($\mathrm{In_{Cu}}$). On the other hand, in the second set, half of the In atoms on the cation-terminated surface become Cu antisites ($\mathrm{Cu_{In}}$) whereas half of the Cu atoms on the anion terminated surface become $\mathrm{In_{Cu}}$. Therefore, the CIS side of the (110) interface can be faceted, where we consider ($2V_{\mathrm{Cu}} + \mathrm{In_{Cu}}$), which is the first set of point defects with a V_{Cu}:$\mathrm{In_{Cu}}$ ratio of 2:1, ($\mathrm{Cu_{In}} + \mathrm{In_{Cu}}$) that is the second set of point defects, and no point defects (simply denoted as faceted), or flat (nonfaceted). The corresponding CdS or ZnS side of the interface is faceted for the first three CIS terminations and nonfaceted for the nonfaceted CIS termination.

The faceted and nonfaceted interfaces and surfaces were treated using a supercell approach. The structure of the supercells for the coherent (110) interfaces and the positions of the point defects are shown in Fig. 1. The CIS, CdS, and ZnS slabs are 11 to 13 layers thick for both interface and surface models. The thickness of the vacuum region corresponds to around nine layers (∼20 Å) for the surface models. Here, Γ-centered k-point meshes of $4 \times 2 \times 1$ and $4 \times 4 \times 1$ were used for calculations with faceted and nonfaceted (110) interfaces or surfaces, respectively, where the former has twice as large an interface or a surface area in the supercell as the latter. Spin polarization was allowed in all calculations. In the interface and surface calculations, the atomic coordinates were obtained using the Hubbard U correction to the generalized gradient approximation (GGA + U) to density functional theory because atomic relaxation using the HSE06 functional is computationally too demanding. The Perdew-Burke-Ernzerhof functional[45] and Dudarev's approach[46] with $U - J = 5$ eV on Cu $3d$ orbitals were used in the GGA + U calculations. The ILPs were first fixed to the GGA + U bulk values, and the atomic coordinates were fully relaxed using the GGA + U. The cell dimension in the out-of-plane (slab stacking or thickness) direction was relaxed for the interfaces while fixed for the surfaces. The ILPs and the cell dimension in the out-of-plane direction were then scaled using HSE06 bulk values with the fractional atomic coordinates fixed to the GGA + U values, and HSE06 calculations were conducted without relaxation of atomic coordinates and cell dimensions. The scaling of the cell dimension in the thickness direction in an interface calculation L was carried out by first determining the mixing m from the GGA + U relaxed cell dimension $L_{\mathrm{GGA}+U}$ and the corresponding cell dimensions $L_{\mathrm{A,GGA}+U}$ and $L_{\mathrm{B,GGA}+U}$ for phases A and B when the entire cell consists of only A or B, respectively:

$$L_{\mathrm{GGA}+U} = mL_{\mathrm{A,GGA}+U} + (1-m)L_{\mathrm{B,GGA}+U}. \quad (1)$$

Next, the scaled HSE06 cell dimension L_{HSE} was obtained by

$$L_{\mathrm{HSE}} = mL_{\mathrm{A,HSE}} + (1-m)L_{\mathrm{B,HSE}}, \quad (2)$$

where $L_{\mathrm{A,HSE}}$ and $L_{\mathrm{B,HSE}}$ are the corresponding HSE06 values. An electrostatic potential averaged within a PAW sphere at each atomic site was taken as the reference level in the evaluation of interfacial band offsets and IPs. The 1:1:2 average of Cu, In, and Se atoms was considered for the reference level of CIS and the 1:1 average of Cd (Zn) and S was used for CdS

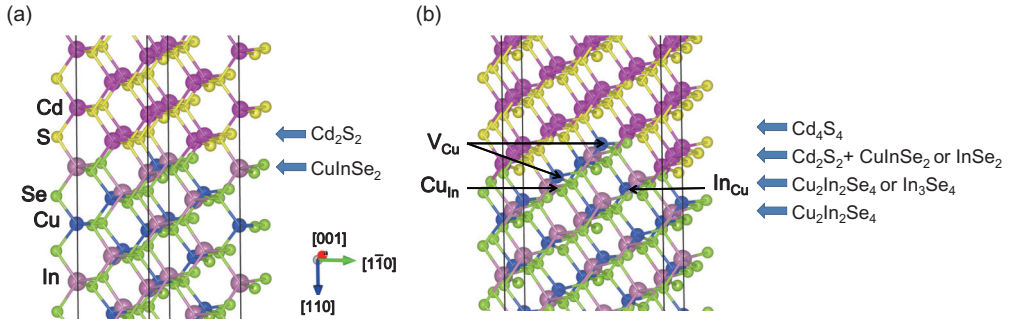

FIG. 1. (Color online) Structure of (a) nonfaceted and (b) faceted CIS/CdS (110) interfaces and the positions of defects necessary to form the $(2V_{Cu} + In_{Cu})$ and $(Cu_{In} + In_{Cu})$ interfaces.

(ZnS). The vacuum level was determined by the local potential in the vacuum region of the surface slab models.

B. Interfacial energy

The stability of interfaces can be evaluated using the interfacial excess energy, which is given per interface supercell as

$$E_{\text{excess}} = E_{\text{interface}} - \sum_i n_i \mu_i, \tag{3}$$

where $E_{\text{interface}}$ is the total energy of an interface supercell, n_i is the number of atoms in the supercell, and μ_i is the chemical potential of atom species i. In the single phase regions of CIS, CdS, and ZnS in the Cu-In-Se ternary, Cd-S binary, and Zn-S binary systems, respectively, the chemical potentials are related as

$$\mu_{Cu} + \mu_{In} + 2\mu_{Se} = \mu_{CIS(bulk)}, \tag{4}$$

$$\mu_{Cd} + \mu_S = \mu_{CdS(bulk)}, \tag{5}$$

$$\mu_{Zn} + \mu_S = \mu_{ZnS(bulk)}, \tag{6}$$

where $\mu_{CIS(bulk)}$, $\mu_{CdS(bulk)}$, and $\mu_{ZnS(bulk)}$ are the chemical potentials for bulk CIS, CdS, and ZnS, corresponding to the total energies per formula unit for these bulk phases. Using Eqs. (3)–(5), the excess energy can be rewritten for the CIS/CdS interface as

$$E_{\text{excess}} = E_{\text{interface}} - \left(\frac{n_{Se}}{2}\mu_{CIS(bulk)} + n_S\mu_{CdS(bulk)} + \Delta n_{Cu}\mu_{Cu} + \Delta n_{In}\mu_{In}\right), \tag{7}$$

where Δn_{Cu} and Δn_{In} are the number of the Cu and In atoms in the interface supercell that are added to the stoichiometric interface to form point defects, respectively. In the portion of the $(2V_{Cu} + In_{Cu})$ interface, three Cu are removed from and one In is added to the stoichiometric interface on one side, which corresponds to $\Delta n_{Cu} = -6$ and $\Delta n_{In} = 2$ in the presence of the two identical interfaces in the supercell. Here, Δn_{Cu} and Δn_{In} are zero for the other interfaces, hence only the excess energy of the $(2V_{Cu} + In_{Cu})$ interface is chemical-potential dependent among the interfaces considered in this work. The range of μ_{Cu} and μ_{In} is constrained within the single phase region of CIS in the Cu-In-Se ternary system reported in Ref. 15, and the surface energy is the lowest when the surface is $(Cu_{In} + In_{Cu})$ or $(2V_{Cu} + In_{Cu})$ in this region. The CdS component of all the interface configurations is stoichiometric ($n_{Cd} = n_S$); therefore, Eq. (7) can be described without μ_{Cd} and μ_S but by using $\mu_{CdS(bulk)}$ only through Eq. (5). The excess energy for the CIS/ZnS interface is given in the same manner. The ILPs for bulk CIS, CdS, and ZnS are set to be equal to that of the interface model to exclude the contribution of in-plane strain to the excess energy when evaluating $\mu_{CIS(bulk)}$, $\mu_{CdS(bulk)}$, and $\mu_{ZnS(bulk)}$.

III. RESULTS AND DISCUSSION

A. Fundamental properties of perfect crystals

The lattice constants a and c, the internal parameter for the Se coordinates u, and the band gap for CIS together with the lattice constants and band gaps for CdS and ZnS obtained by GGA($+U$) and HSE06 are summarized in Table I. Here, GGA($+U$) significantly underestimates the band gaps for all of CIS, CdS, and ZnS. In particular, the band gap of CIS is very small at around 0.1 eV, which makes it difficult to discuss in-gap electronic states at the interface. A noticeable improvement is found with HSE06 ($a = 0.25$), but underestimation still

TABLE I. Calculated and experimental structural parameters (the lattice constants a and c and the internal parameter u) and band gap (E_g) for CIS with the chalcopyrite structure and for ZnS and CdS with the zincblende structure. The GGA+U values are shown for CIS while the GGA values for CdS and ZnS in the GGA($+U$) column.

		GGA($+U$)	HSE06 ($a = 0.25$)	HSE06 ($a = 0.30$)	Experiment
CIS	a (Å)	5.878	5.845	5.837	5.784[a]
	c (Å)	11.828	11.756	11.730	11.616[a]
	u	0.221	0.225	0.227	0.224[a]
	E_g (eV)	0.08	0.78	1.04	1.05[b]
CdS	a (Å)	5.927	5.886	5.879	5.818[c]
	E_g (eV)	1.06	2.13	2.35	2.46[d]
ZnS	a (Å)	5.444	5.423	5.419	5.409[e]
	E_g (eV)	2.03	3.29	3.55	3.73[d]

[a]Reference 53.
[b]Reference 54.
[c]Reference 55.
[d]Reference 56.
[e]Reference 57.

prevails for all the systems. The HSE06 ($a = 0.30$) reproduces the band gap of CIS very well and, simultaneously, the band gaps of CdS and ZnS become much closer to the experimental values. In addition, the lattice constants are best described with HSE06 ($a = 0.30$) for all compounds, which is preferable for the investigation of the strain effects on the band offsets. Only the results with $a = 0.30$ are shown hereafter; calculations were systematically performed with both $a = 0.25$ and 0.30, and the band offsets with $a = 0.25$ and 0.30 were found to differ typically by less than 0.03 eV.

B. Critical thickness for the coherent to semicoherent transition of the interface

The CIS/CdS and CIS/ZnS interfaces are expected to have coherent structures or semicoherent structures with misfit dislocations because of the similarity in crystal structures between CIS and CdS or ZnS. The derivation by Matthews and Blakeslee[47] based on mechanical equilibrium gives the critical thickness h_c of a strained thin film as

$$ph_c = \frac{b}{qf}\left[\ln\left(\frac{ph_c}{b}\right) + 1\right], \tag{8}$$

where b is the length of the Burgers vector and f is the lattice misfit. The coefficients are $p = 4$ for a single epitaxial film on a substrate of infinite thickness and $q = 2\pi(1+\nu)\cos\lambda/(1-\nu^2\cos^2\alpha)$, where ν is the Poisson ratio, α is the angle between the dislocation line and its Burgers vector, and λ is the angle between the slip direction and the direction in the film plane perpendicular to the line of intersection of the slip plane and the interface. The solution to Eq. (8) is given using Lambert's W function as

$$\frac{h_c}{b} = \frac{-1}{fpq} W\left(\frac{-fq}{e}\right), \tag{9}$$

where e is Napier's constant. Here, we consider an edge ($\cos\alpha = 0$) dislocation with a Burgers vector of $\frac{a}{2}\langle 1\bar{1}0\rangle$ and $\lambda = 0$, and a typical Poisson ratio of $\nu = 1/3$ is assumed. The length of the Burgers vector ($\sqrt{2}a/2$) is equal to twice the thickness of a (110) monolayer ($\sqrt{2}a/4$). In other words, the thickness of a monolayer is $b/2$. Figure 2 shows a plot of the critical thickness normalized by the (110) monolayer thickness, $h_c/(b/2)$, versus the lattice misfit f.

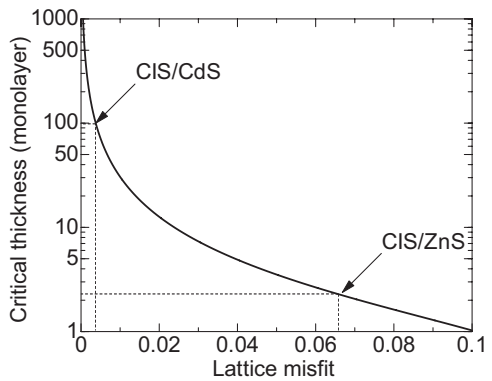

FIG. 2. Critical thickness of a film epitaxially grown on the (110) surface versus lattice misfit for chalcopyrite/zincblende systems estimated using the formulation by Matthews and Blakeslee.[47]

Using the experimental lattice constants, the lattice misfit of CdS against CIS averaged on the (110) plane is $f_{\mathrm{CdS/CIS}} = |\sqrt{2a_{\mathrm{CdS}}^2/(a_{\mathrm{CIS}}c_{\mathrm{CIS}})} - 1| = 0.004$, and the corresponding misfit of ZnS against CIS is $f_{\mathrm{ZnS/CIS}} = 0.067$. The resultant critical thickness for CIS/CdS is about 100 layers, whereas that of CIS/ZnS is about two layers, which implies that the coherent interface for CIS/ZnS does not commonly form. However, the band offset of a coherent CIS/ZnS interface is considered as well as that of a coherent CIS/CdS interface in this study to systematically investigate the effects of lattice strain on the band offset by calculating the interfaces with various ILPs, that is, either those of CIS, ZnS, or CdS, or the average of CIS and ZnS or CdS.

C. Interfacial energy

The excess energies excluding strain contributions for the coherent CIS/CdS and CIS/ZnS interfaces with various ILPs are listed in Table II. The energies are normalized to the values per 1 Å^2 area of the (110) interface plane for both faceted and nonfaceted interfaces. The range of the excess energies for the $(2V_{\mathrm{Cu}} + \mathrm{In_{Cu}})$ interface corresponds to the chemical potential range of Cu and In allowed in the CIS single phase region in the Cu-In-Se ternary system.[15] The excess energies of the interfaces without point defects, namely the nonfaceted and faceted interfaces, are 0.7–3.5 meV/Å^2, whereas those for the $(2V_{\mathrm{Cu}} + \mathrm{In_{Cu}})$ and $(\mathrm{Cu_{In}} + \mathrm{In_{Cu}})$ interfaces are 7.9–30.9 meV/Å^2 and 11.3–14.6 meV/Å^2, respectively. The faceted interfaces without point defects show similar energies to the nonfaceted interfaces despite the fact that the interfacial area is increased by the formation of the facets from a microscopic viewpoint. Furthermore, the existence of a high concentration of ordered point defects at the interfaces is clearly unfavorable irrespective of the ILPs and chemical potentials, which contrasts with the tendency where the energy is lowered by forming facets and point defects at the (110) surface in CIS.[15,24] However, the interfaces with such ordered point defects may form, for instance, when CdS or ZnS films are deposited onto the stable CIS surfaces with ordered point defects at low temperature. We therefore show the results for the interfaces with ordered point defects as well as the stable interfaces without point defects in the following sections on the band offsets.

D. Electronic states near the interface

Figure 3 shows the site projected electronic density of states (DOS) for each layer in CIS/CdS supercells with CIS ILPs. The DOS per one layer of a faceted interface supercell, which consists of eight atoms if there are no vacancies, is given. Figure 3(a) shows the DOS for the nonfaceted interface. The number of atoms in one layer of the nonfaceted interface supercell is four and, therefore, the DOS are normalized accordingly. There are no clear interface states in the CIS region. On the other hand, in the CdS region, there are interface states composed mainly of S $3p$ orbitals at two layers from the interface between about -1 to 0 eV from the highest occupied state in the interface supercell ($\varepsilon_{\mathrm{HOS}}$). These states result from the hybridization with Cu $3d$ states that mainly constitute the upper part of the valence band of CIS. Similar interface states

TABLE II. Excess energies excluding strain contributions for coherent CIS/CdS and CIS/ZnS interfaces with various ILPs. Energies in meV/Å^2.

	CIS/CdS			CIS/ZnS		
	CIS ILP	Average ILP	CdS ILP	CIS ILP	Average ILP	ZnS ILP
Nonfaceted	2.4	2.4	2.4	2.1	2.0	3.3
Faceted	1.6	2.2	2.1	0.7	2.1	3.5
$(2V_{Cu} + In_{Cu})$	9.1–28.8	9.6–29.2	9.5–29.0	9.0–28.7	9.5–30.7	7.9–30.9
$(Cu_{In} + In_{Cu})$	12.3	12.8	12.7	11.3	13.3	14.6

are visible in the faceted interface [Fig. 3(b)], implying that the nonfaceted and faceted interfaces are very similar regarding the electronic structure at the interface. The band offset is also about the same in these two interfaces, as shown later.

In the DOS for the $(2V_{Cu} + In_{Cu})$ interface [Fig. 3(c)], the highest occupied state of CIS at the interface has lower energy than the VBM given by the center of the CIS slab, and there is an interface state in the CdS region localized at one layer below the interface at about −0.8 eV from ε_{HOS}. In contrast, the DOS for the $(Cu_{In} + In_{Cu})$ interface in Fig. 3(d) has occupied interface states at the top of the valence band of CIS that distribute up to approximately 0.4 eV above the

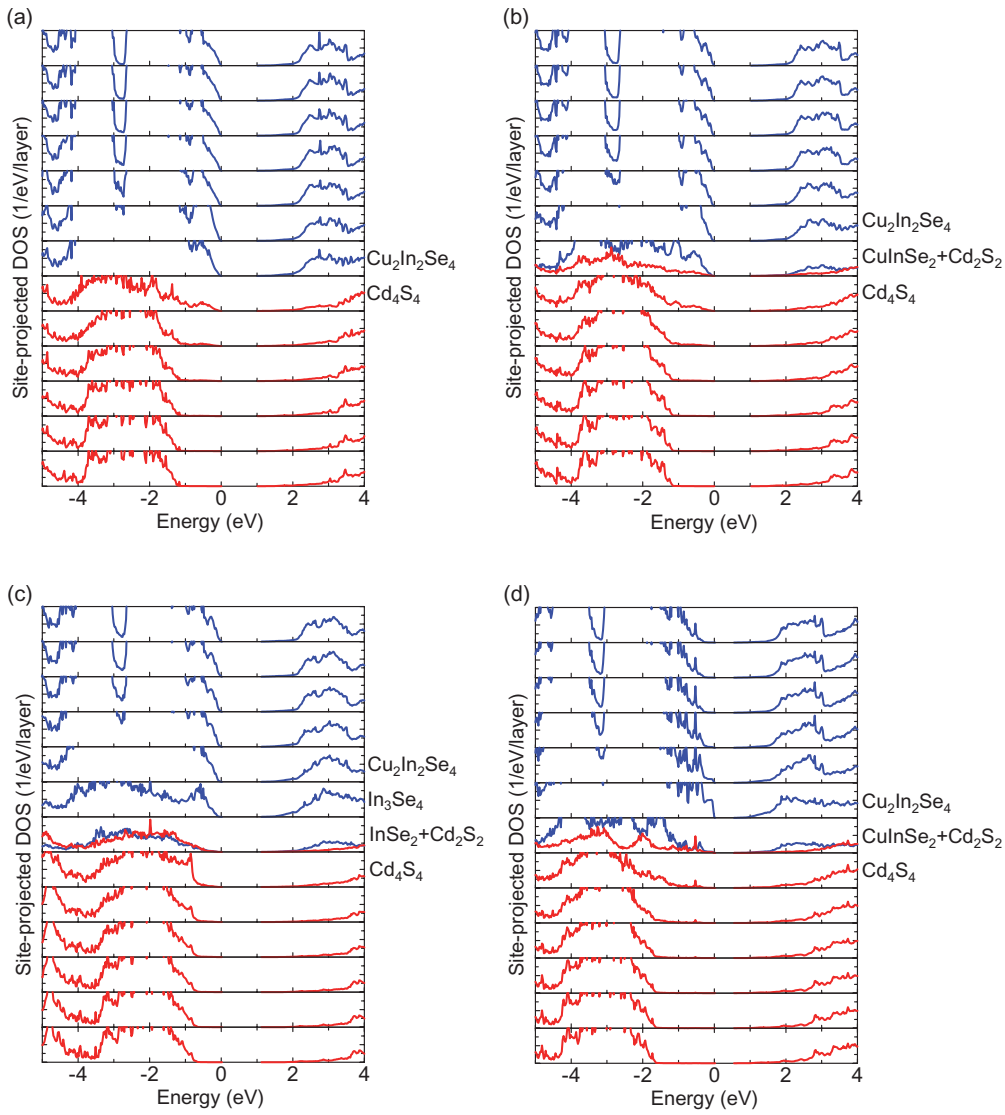

FIG. 3. (Color online) Site-projected DOS for each layer of the CIS/CdS interface supercells with CIS ILPs from the center of the CIS slab (top) to the center of the CdS slab (bottom). Interfaces are (a) nonfaceted, (b) faceted, (c) $(2V_{Cu} + In_{Cu})$, and (d) $(Cu_{In} + In_{Cu})$. Energies are taken against the highest occupied state in each supercell. The DOS is per layer consisting of eight atoms unless otherwise shown, and one notch corresponds to 1/eV/layer. The blue and red curves denote DOS for CIS and CdS, respectively.

TABLE III. Strained valence band offsets for CIS/CdS and CIS/ZnS interfaces with various ILPs. Values with respect to CIS are shown in eV.

	CIS/CdS			CIS/ZnS		
	CIS ILP	Average ILP	CdS ILP	CIS ILP	Average ILP	ZnS ILP
Nonfaceted	−1.16	−1.18	−1.20	−1.08	−1.40	−1.75
Faceted	−1.15	−1.17	−1.19	−1.07	−1.41	−1.75
$(2V_{Cu} + In_{Cu})$	−0.74	−0.76	−0.78	−0.64	−0.96	−1.28
$(Cu_{In} + In_{Cu})$	−1.20	−1.22	−1.23	−1.13	−1.45	−1.78

VBM determined by the bulklike region of the CIS side. These states are formed by Cu $3d$ and Se $4p$ orbitals and are mostly localized on the second layer that includes Cu_{In} and In_{Cu}. The $(112)/(11\bar{2})$ faceted surface of CIS with ordered $(Cu_{In} + In_{Cu})$ defects has similar electronic states.[15] In addition, there are interface states in the CdS region, which are composed of S $3p$ orbitals at the interface and two subsequent layers.

E. Valence band offsets

Different band offsets are appropriate in the following two scenarios. The strained band offset is relevant when the ILPs are the same in the two phases. A typical example is a coherent interface formed when a thin film of a second phase below the critical thickness is epitaxially grown on a thick substrate. In contrast, the natural band offset is necessary when both phases constituting the interface can relax to their ideal lattice parameters, for instance by forming a semicoherent interface with misfit dislocations or an incoherent interface. These two band offsets both have physical meanings, which motivate exploration of methods to calculate these quantities.

Three types of calculations can be used to obtain three types of energy level differences. First, bulk calculations provide the energy difference from a reference level to the VBM for a phase A with ILPs of phase X, $\Delta\varepsilon^{A}_{VBM\text{-}Ref,X} = \varepsilon^{A}_{VBM,X} - \varepsilon^{A}_{Ref,X}$. For example, if we are interested in a thin film of CIS below critical thickness on a CdS substrate with a (110) interface, one important quantity is $\Delta\varepsilon^{CIS}_{VBM\text{-}Ref,CdS} = \varepsilon^{CIS}_{VBM,CdS} - \varepsilon^{CIS}_{Ref,CdS}$, which is the energy difference in CIS (=A) with CdS (=X) ILPs perpendicular to the [110] direction. Second, surface calculations are used to obtain the energy difference from a reference level near the center of a slab to the vacuum level for a phase A with ILPs of phase X, $\Delta\varepsilon^{A}_{Vac\text{-}Ref,X} = \varepsilon_{Vac} - \varepsilon^{A}_{Ref,X}$. This is necessary to determine the absolute position of the reference level because the reference level in an infinitely extending bulk is ill-defined.[48] Finally, interface calculations give the difference between reference levels near the center of slabs of two phases A and B, $\Delta\varepsilon^{A\text{-}B}_{Ref,X} = \varepsilon^{A}_{Ref,X} - \varepsilon^{B}_{Ref,X}$. The ILPs perpendicular to the thickness direction can be anything (=X), but geometrically must be the same in phases A and B. The strained and natural valence band offsets are obtained by adding and subtracting these energy level differences.

1. Strained band offset

The strained band offset [Fig. 4(a)] uses one interface and two bulk calculations. The ILPs are fixed to a common set X in all calculations, and the other lattice parameters and internal coordinates are optimized. The resulting offset is

$$\Delta\varepsilon^{A\text{-}B,strained}_{VBM,X} = \Delta\varepsilon^{A}_{VBM\text{-}Ref,X} + \Delta\varepsilon^{A\text{-}B}_{Ref,X} - \Delta\varepsilon^{B}_{VBM\text{-}Ref,X}. \quad (10)$$

The I-shaped bars in Fig. 4(a) indicate energy level differences from bulk calculations, and the difference in the reference levels of two phases $\Delta\varepsilon^{A\text{-}B}_{Ref,X}$ is determined by a coherent interface calculation. Note that the two phases need not contain a common element because the reference levels are independently taken in the respective phases.

The strained band offsets with respect to CIS are summarized in Table III. The VBM of CdS and ZnS is lower compared to that of CIS in all cases (negative values in Table III). The strained band offset varies widely with the ILPs when the lattice misfit is large; this quantity varies by about 0.7 eV for the CIS/ZnS interface that has a large lattice misfit (∼7%). The decrease in the band offset, or relative heightening of the ZnS VBM with respect to the CIS VBM, when the ILPs are decreased from those of CIS to ZnS, is accompanied by a broadening by about 0.5 eV of the Cu $3d$ band immediately below the VBM. The strained band offsets are essentially independent of the structure of the interface, with one exception of the $(2V_{Cu} + In_{Cu})$ interface when compared within the same ILPs. The absolute value of the strained band offset of the $(2V_{Cu} + In_{Cu})$ interface is about 0.4 eV smaller. This energy difference can be explained by the dipole moment associated with charged layers at the interface as discussed below.

The $(2V_{Cu} + In_{Cu})$ interface is composed of In_3Se_4 and $InSe_2 + Cd_2S_2$ or $InSe_2 + Zn_2S_2$ (110) layers as shown in Fig. 1(b). Assuming the formal charges of +3 for In, +2 for Cd and Zn, and −2 for Se and S, these layers have net charges of +1 and −1, respectively, in a supercell with a cross-section of $A \approx 90$ Å^2. All other layers are charge neutral. Analysis of the DOS [Fig. 3(c)] shows that V_{Cu} and In_{Cu} compensate each other as single acceptors in charge state −1 and double donors in charge state +2, respectively. The electrostatic potential at this interface can be modeled as a parallel-plate capacitor, and the potential difference over the interface is estimated as $\Delta V = ed/(\varepsilon_0\varepsilon_r A)$, where e is the elementary positive charge and ε_0 is the permittivity of vacuum. The interlayer distance d is about 2 Å, and the static dielectric constant of CIS ε_r is reported as 11.1,[49] 13.6,[50] and 16.63,[50] which results in a potential difference of about 0.3 V over the interface. Thus, the potential drop at the interface can be explained by the existence of charged layers. In contrast, the $(Cu_{In} + In_{Cu})$ interface has formally neutral (110) layers only because Cu_{In} and In_{Cu} located on the same layer compensate each other as double

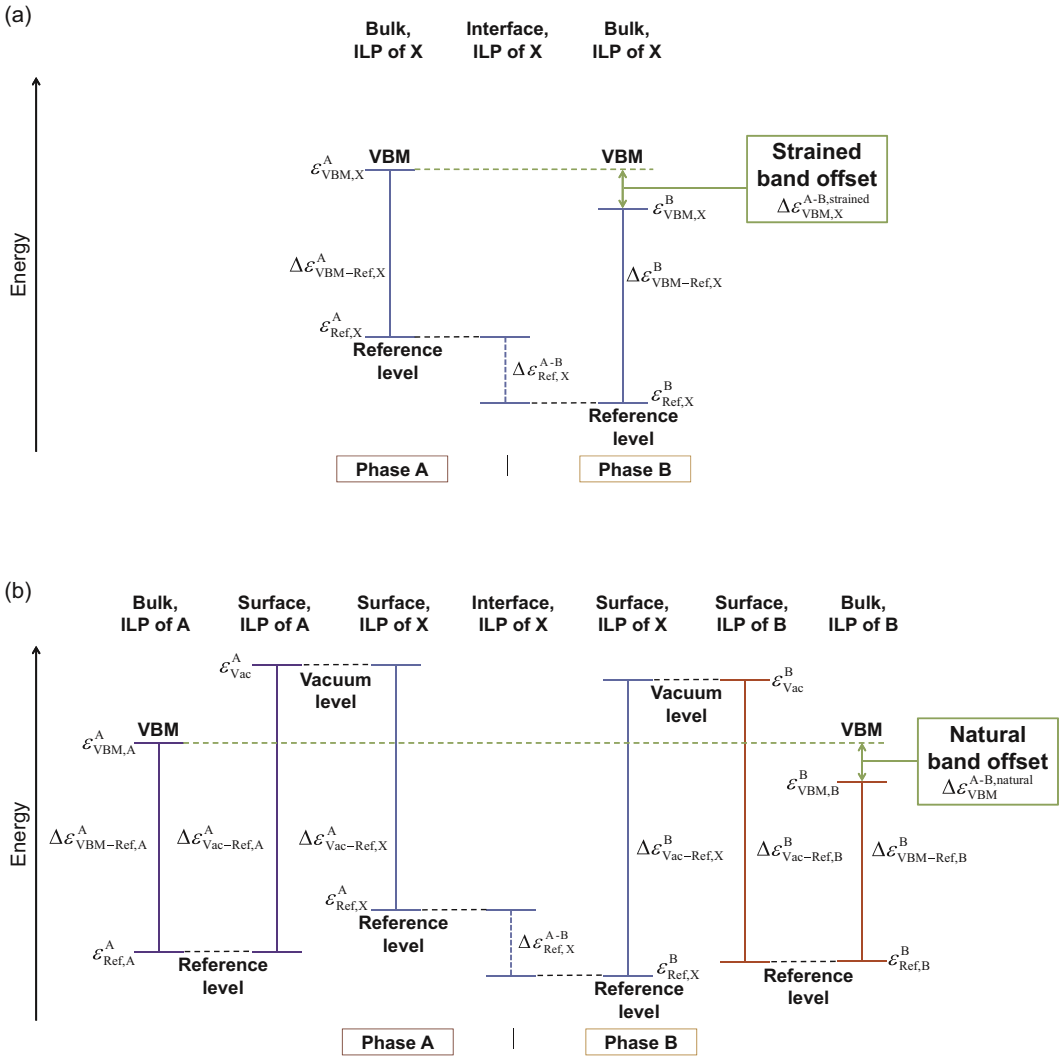

FIG. 4. (Color online) Alignment of energy levels to obtain the (a) strained and (b) natural valence band offset.

acceptors in charge state −2 and double donors in charge state +2, respectively. The valence band offset at the $(Cu_{In} + In_{Cu})$ interface is very similar to those of the nonfaceted and faceted interfaces without point defects, although the ordered defects cause significant deviations of the reference levels in their vicinity as mentioned below.

Figure 5 shows the reference levels of the constituent atoms in CIS/CdS interface models with CIS ILPs. The reference levels with respect to the highest occupied level ε_{HOS} for each atom $\varepsilon^{i}_{Ref,CIS} - \varepsilon_{HOS} = \Delta\varepsilon^{i}_{Ref\text{-}HOS,CIS}$ (i = Cu, In, Se) in CIS and $\varepsilon^{j}_{Ref,CIS} - \varepsilon_{HOS} = \Delta\varepsilon^{j}_{Ref\text{-}HOS,CIS}$ (j = Cd, S) in CdS are shifted by the relevant difference between the VBM and the reference level for each atom in bulk CIS or CdS $\Delta\varepsilon^{i}_{VBM\text{-}Ref,CIS}$ or $\Delta\varepsilon^{j}_{VBM\text{-}Ref,CIS}$ with CIS ILPs. In other words, the quantities $\Delta\varepsilon^{i}_{Ref\text{-}HOS,CIS} + \Delta\varepsilon^{i}_{VBM\text{-}Ref,CIS}$ and $\Delta\varepsilon^{j}_{Ref\text{-}HOS,CIS} + \Delta\varepsilon^{j}_{VBM\text{-}Ref,CIS}$ are shown. The reference levels of Cu, In, and Se ultimately converge to a fixed quantity far from the interface. The interface regions, where the reference levels of atoms clearly deviate from the converged values, are about two layers for both CIS and CdS in the nonfaceted [Fig. 5(a)] and faceted [Fig. 5(b)] interfaces, and four layers for CIS and three layers for CdS in the $(2V_{Cu} + In_{Cu})$ [Fig. 5(c)] and $(Cu_{In} + In_{Cu})$ [Fig. 5(d)] interfaces. The zero energy in Fig. 5 corresponds to the highest occupied state, which is the VBM of CIS for the nonfaceted, faceted, and $(2V_{Cu} + In_{Cu})$ interfaces. The exception is the $(Cu_{In} + In_{Cu})$ interface [Fig. 5(d)], where the zero energy is at an interface state. There are occupied interface states at the $(Cu_{In} + In_{Cu})$ interface up to approximately 0.4 eV above the bulk CIS VBM as shown in Fig. 3(d), which agrees with the shift of about −0.4 eV in the bulk CIS VBM from ε_{HOS} in Fig. 5(d).

An alternative method to estimate the strained band offset is to use the strained IP difference between strained surfaces defined as

$$\Delta\varepsilon^{\text{A-B,strained}}_{IP,X} = \left(\Delta\varepsilon^{A}_{VBM\text{-}Ref,X} - \Delta\varepsilon^{A}_{Vac\text{-}Ref,X}\right) - \left(\Delta\varepsilon^{B}_{VBM\text{-}Ref,X} - \Delta\varepsilon^{B}_{Vac\text{-}Ref,X}\right). \quad (11)$$

A bulk calculation and a surface calculation of a unit cell containing a slab of one phase and a vacuum region yield the value in one bracket in Eq. (11), which is equal to the negative of the IP. The IP values excluding the surface state effects as much as possible are appropriate for interfacial band offset

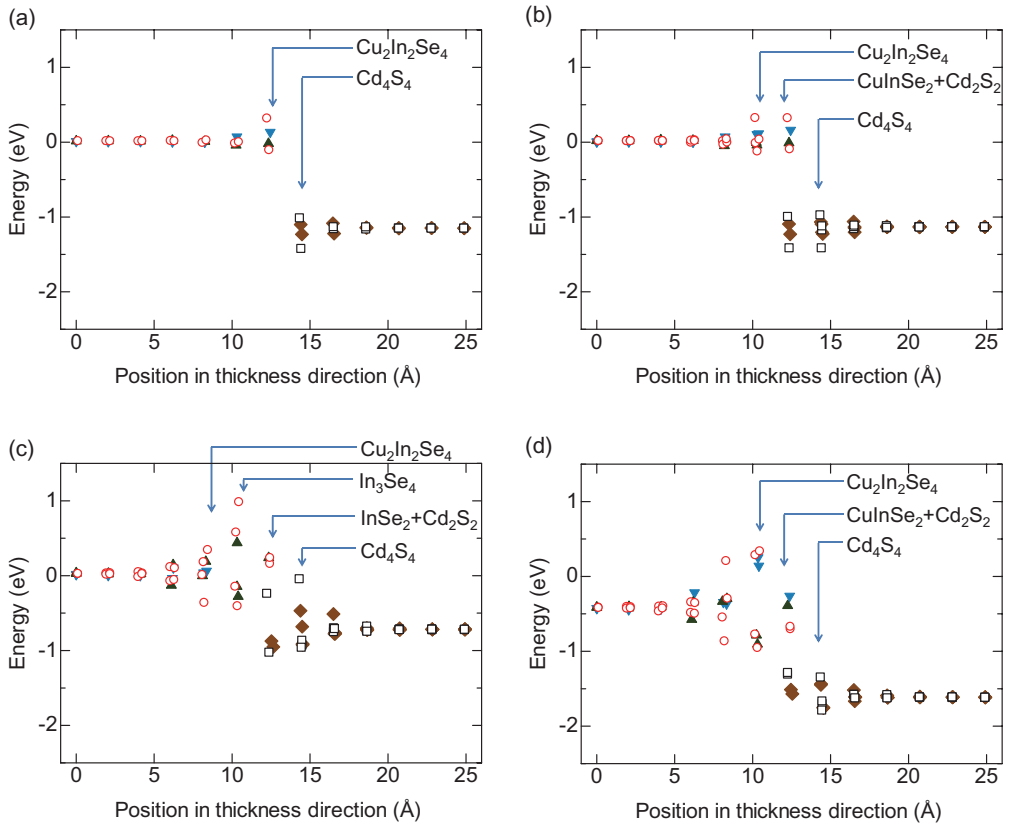

FIG. 5. (Color online) Reference levels of the constituent atoms in CIS/CdS interface models with CIS ILPs. The quantities $\Delta\varepsilon^{i}_{\text{Ref-HOS,CIS}} + \Delta\varepsilon^{i}_{\text{VBM-Ref,CIS}}$ (i = Cu, In, Se) and $\Delta\varepsilon^{j}_{\text{Ref-HOS,CIS}} + \Delta\varepsilon^{j}_{\text{VBM-Ref,CIS}}$ (j = Cd, S) are shown for (a) nonfaceted, (b) faceted, (c) $(2V_{\text{Cu}} + \text{In}_{\text{Cu}})$, and (d) $(\text{Cu}_{\text{In}} + \text{In}_{\text{Cu}})$ interfaces. The zero energy corresponds to the highest occupied state. Legend: down-pointing blue filled triangles: Cu; up-pointing green filled triangles: In; red circles: Se; brown filled diamonds: Cd; and black squares: S.

estimation purposes, and hence, we utilize the bulk-based IP defined in Ref. 15. To make a comparison with strained band offsets, three choices for ILP X to calculate the IPs of the two phases are considered: that of phase A, phase B, and the average of the two phases. Table IV shows the strained IP differences. The strained band offsets (Table III) and strained IP differences (Table IV) differ by less than about 0.2 eV for the nonfaceted and faceted interfaces without point defects, but differ by a larger amount (up to 0.5 eV) in faceted interfaces with defects. In general, relaxation of atoms and electron charge differ between surfaces and interfaces, and, therefore, the constant shifts in the electrostatic potential caused by the interface and surface dipoles are different. The dipoles also change with in-plane strain because of changes in the density of atoms and electron charge. The band offset and the IP difference become similar only when the difference in surface dipoles between two phases is similar to the interface dipole. This seems to hold for the nonfaceted and faceted interfaces without point defects.

2. *Natural band offset*

The strained band offset is appropriate for a coherent interface with lattice strain. However, ILPs relax if the film thickness on one side of the interface exceeds a critical thickness, and the effects from this relaxation should be taken into account in this case. This correction may be made using surface calculations, where the vacuum levels are aligned in

TABLE IV. Strained IP differences obtained from CIS, CdS, and ZnS surfaces with various ILPs. Values corresponding to the coherent interface valence band offsets with respect to CIS are shown in eV. The value for the faceted CIS/ZnS interface with the ZnS ILP is excluded because the strained CIS surface used in the derivation had an unreasonably small band gap.

	CIS/CdS			CIS/ZnS		
	CIS ILP	Average ILP	CdS ILP	CIS ILP	Average ILP	ZnS ILP
Nonfaceted	−1.05	−1.07	−1.08	−1.04	−1.35	−1.76
Faceted	−1.05	−1.07	−1.09	−1.01	−1.32	
$(2V_{\text{Cu}} + \text{In}_{\text{Cu}})$	−1.04	−1.05	−1.06	−1.01	−1.42	−1.84
$(\text{Cu}_{\text{In}} + \text{In}_{\text{Cu}})$	−1.41	−1.43	−1.44	−1.38	−1.81	−2.30

TABLE V. Natural valence band offsets for CIS/CdS and CIS/ZnS interfaces with various ILPs. Values with respect to CIS are shown in eV. The offset of the faceted CIS/ZnS interface with the ZnS ILP is excluded because the strained CIS surface used in the derivation had an unreasonably small band gap.

	CIS/CdS			CIS/ZnS		
	CIS ILP	Average ILP	CdS ILP	CIS ILP	Average ILP	ZnS ILP
Nonfaceted	−1.20	−1.20	−1.20	−1.27	−1.28	−1.22
Faceted	−1.18	−1.18	−1.19	−1.28	−1.32	
$(2V_{Cu} + In_{Cu})$	−0.78	−0.78	−0.79	−0.85	−0.76	−0.66
$(Cu_{In} + In_{Cu})$	−1.23	−1.23	−1.24	−1.34	−1.23	−1.07

two surface calculations with ILP X and A or B. Here, a total of seven calculations, which include four surface calculations to correct the ILPs, are employed to derive the natural band offset as illustrated in Fig. 4(b). The natural band offset is defined as

$$\Delta\varepsilon^{\text{A-B,natural}}_{\text{VBM}} = \left(\Delta\varepsilon^{\text{A}}_{\text{VBM-Ref,A}} - \Delta\varepsilon^{\text{A}}_{\text{Vac-Ref,A}} + \Delta\varepsilon^{\text{A}}_{\text{Vac-Ref,X}}\right) + \Delta\varepsilon^{\text{A-B}}_{\text{Ref,X}} - \left(\Delta\varepsilon^{\text{B}}_{\text{VBM-Ref,B}} - \Delta\varepsilon^{\text{B}}_{\text{Vac-Ref,B}} + \Delta\varepsilon^{\text{B}}_{\text{Vac-Ref,X}}\right). \quad (12)$$

This is similar to that used by Lany *et al.*[23] in the sense that the difference between IPs of the same phase with different ILPs are used. The values for the natural band offsets are shown in Table V. The natural band offset should, in principle, be independent of the ILPs that were used for the interface calculations. However, this is not the case for the CIS/ZnS interface that has a large lattice misfit. The absolute value of the natural band offset for the CIS/ZnS interface decreases gradually when the ILPs are decreased from that of CIS to ZnS, implying that the correction for the effects of ILPs on the band offset using surface calculations includes this level of ambiguity.

Figure 6 shows the relative positions of the VBM (sign-inverted bulk-based IP: $\Delta\varepsilon^{\text{CIS}}_{\text{VBM-Ref,X}} - \Delta\varepsilon^{\text{CIS}}_{\text{Vac-Ref,X}}$ and $\Delta\varepsilon^{\text{ZnS}}_{\text{VBM-Ref,X}} - \Delta\varepsilon^{\text{ZnS}}_{\text{Vac-Ref,X}}$) and the relative reference levels $[-\Delta\varepsilon^{\text{CIS}}_{\text{Vac-Ref,X}} - (-\Delta\varepsilon^{\text{CIS}}_{\text{Vac-Ref,CIS}})$ and $-\Delta\varepsilon^{\text{ZnS}}_{\text{Vac-Ref,X}} - (-\Delta\varepsilon^{\text{ZnS}}_{\text{Vac-Ref,ZnS}})]$ in nonfaceted CIS and ZnS surfaces with the CIS, ZnS, and average (=X) ILPs when the vacuum level is aligned. The shift in the reference level versus the vacuum level changes nonlinearly with respect to the lattice parameter, which is particularly evident in CIS. The reference level versus the vacuum level $(-\Delta\varepsilon^{\text{A}}_{\text{Vac-Ref,X}})$ is less dependent on the in-plane lattice parameter than the VBM versus the vacuum level $(\Delta\varepsilon^{\text{A}}_{\text{VBM-Ref,X}} - \Delta\varepsilon^{\text{A}}_{\text{Vac-Ref,X}})$ and the VBM versus the reference level $(\Delta\varepsilon^{\text{A}}_{\text{VBM-Ref,X}})$. The variation in the reference level difference between CIS and ZnS, $\Delta\varepsilon^{\text{CIS}}_{\text{Vac-Ref,X}} - \Delta\varepsilon^{\text{ZnS}}_{\text{Vac-Ref,X}}$, is within 0.10 eV over a lattice mismatch of about 7% between X = CIS and X = ZnS. This quantity increases to 0.21 eV for $(2V_{Cu} + In_{Cu})$ and 0.29 eV for $(Cu_{In} + In_{Cu})$. Regarding the faceted surface, the CIS surface with the ZnS ILP results in an unreasonably small band gap, and therefore we cannot provide the corresponding value. The difference between CIS and average ILPs of this surface is less than 0.01 eV, which is as small as that of the nonfaceted surface shown in Fig. 6. We found that the ILP dependence of the reference level difference between CIS and ZnS in the interface model $\Delta\varepsilon^{\text{CIS-ZnS}}_{\text{Ref,X}}$ is even weaker, and the variation is within 0.05, 0.05, 0.01, and 0.03 eV for the nonfaceted, faceted, $(2V_{Cu} + In_{Cu})$, and $(Cu_{In} + In_{Cu})$ interfaces, respectively.

The shift of the electrostatic potential or core level as a reference level with respect to changes in lattice parameters is considered important when using absolute deformation potentials to correct for the changes in ILPs.[20–22] The reference level shift may be larger when using absolute deformation potentials because calculation of an abrupt homointerface at fixed lattice parameters and internal coordinates is inevitable in derivation of absolute deformation potentials, resulting in an unnaturally strained state. In contrast, our bulk, surface, and interface calculations allow relaxation of the cells along one direction while fixing the ILPs, and all internal coordinates are also allowed to relax. The weak ILP dependence of the reference level difference suggests not carrying out the surface calculations for the estimation of the reference level shift because the use of surface calculations can be a source of error by itself; the local dipole moments at the surfaces with different ILPs cannot completely cancel out. The simplified natural band

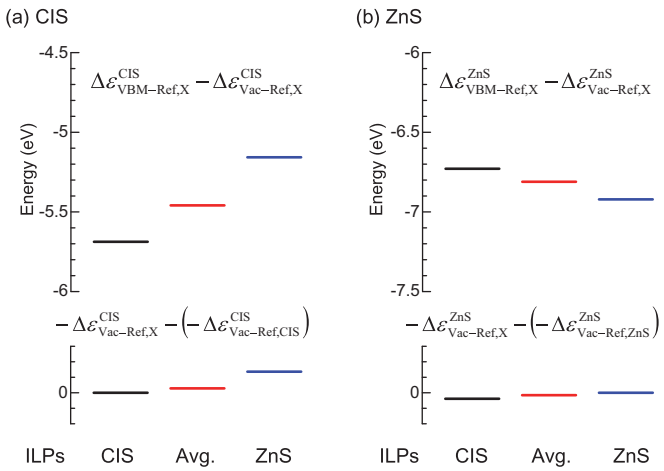

FIG. 6. (Color online) Alignment of energy levels for (a) CIS and (b) ZnS when the in-plane lattice parameters (ILPs) are either that of CIS, the average of CIS and ZnS, or that of ZnS. The sign-inverted bulk-based IPs $(\Delta\varepsilon^{\text{CIS}}_{\text{VBM-Ref,X}} - \Delta\varepsilon^{\text{CIS}}_{\text{Vac-Ref,X}}$ and $\Delta\varepsilon^{\text{ZnS}}_{\text{VBM-Ref,X}} - \Delta\varepsilon^{\text{ZnS}}_{\text{Vac-Ref,X}})$ and relative reference levels $[-\Delta\varepsilon^{\text{CIS}}_{\text{Vac-Ref,X}} - (-\Delta\varepsilon^{\text{CIS}}_{\text{Vac-Ref,CIS}})$ and $-\Delta\varepsilon^{\text{ZnS}}_{\text{Vac-Ref,X}} - (-\Delta\varepsilon^{\text{ZnS}}_{\text{Vac-Ref,ZnS}})]$ are shown for nonfaceted surfaces. Only the relative values are relevant for the reference level. One notch corresponds to 0.1 eV.

TABLE VI. Simplified natural valence band offsets for CIS/CdS and CIS/ZnS interfaces with various ILPs. Values with respect to CIS are shown in eV.

	CIS/CdS			CIS/ZnS		
	CIS ILP	Average ILP	CdS ILP	CIS ILP	Average ILP	ZnS ILP
Nonfaceted	−1.20	−1.20	−1.20	−1.31	−1.33	−1.36
Faceted	−1.18	−1.19	−1.19	−1.30	−1.34	−1.35
$(2V_{Cu} + In_{Cu})$	−0.78	−0.78	−0.78	−0.87	−0.88	−0.88
$(Cu_{In} + In_{Cu})$	−1.23	−1.23	−1.23	−1.36	−1.37	−1.39

offset is considered in this context, which is defined as

$$\Delta\varepsilon_{\mathrm{VBM}}^{\mathrm{A\text{-}B,natural,simplified}} = \Delta\varepsilon_{\mathrm{VBM\text{-}Ref,A}}^{\mathrm{A}} - \Delta\varepsilon_{\mathrm{VBM\text{-}Ref,B}}^{\mathrm{B}} + \Delta\varepsilon_{\mathrm{Ref,X}}^{\mathrm{A\text{-}B}}, \quad (13)$$

where the terms from surface calculations are omitted from Eq. (12). Table VI shows the simplified natural band offsets, which are almost independent of the ILPs in the interface calculations for both CIS/CdS and CIS/ZnS. The values in Table VI are very close to the natural band offsets (Table V) with any ILPs for the CIS/CdS interfaces, which is obvious because of the small lattice misfit between CIS and CdS. The simplified natural band offset of CIS/CdS for the nonfaceted interface, which is −1.20 eV, is close to a value of −1.07 eV obtained by Wei and Zunger[51] based on a similar procedure but using the LDA calculations. The simplified natural band offsets for the CIS/ZnS interfaces (Table VI) are close to the natural band offsets with CIS and average ILPs (Table V), where the shift of the reference levels from their positions with the bulk ILPs are small, as shown for the nonfaceted surfaces in Fig. 6. The small ILP dependence of the simplified natural band offset means that the surface calculations are indeed causing the overcorrections, and the simplified natural band offset may be more suitable for the prediction of the natural band offset.

Ionization potentials can be used to estimate natural band offsets as in the case of the strained band offsets, and the relevant quantity is the natural IP difference defined as

$$\Delta\varepsilon_{\mathrm{IP}}^{\mathrm{A\text{-}B,natural}} = \left(\Delta\varepsilon_{\mathrm{VBM\text{-}Ref,A}}^{\mathrm{A}} - \Delta\varepsilon_{\mathrm{Vac\text{-}Ref,A}}^{\mathrm{A}}\right) - \left(\Delta\varepsilon_{\mathrm{VBM\text{-}Ref,B}}^{\mathrm{B}} - \Delta\varepsilon_{\mathrm{Vac\text{-}Ref,B}}^{\mathrm{B}}\right). \quad (14)$$

This is simply the difference in the bulk-based IPs of two phases, each with optimized lattice parameters and internal coordinates. The bulk-based IP of CIS is 5.69 (nonfaceted), 5.79 (faceted), 5.79 ($2V_{Cu} + In_{Cu}$), and 5.42 eV ($Cu_{In} + In_{Cu}$), whereas that of CdS is 6.77 (nonfaceted) and 6.87 eV (faceted) and that of ZnS is 6.92 (nonfaceted) and 7.01 eV (faceted). The natural IP differences summarized in Table VII differ significantly from the simplified natural band offsets (Table VI) by up to 0.3 eV. Furthermore, there is no consistent overestimation or underestimation of one over the other. Thus, the prediction accuracy of the natural band offsets using IP differences is limited as in the case of the strained band offsets.

3. *Comparison with experimental valence band offsets*

There are a number of experimental CIS/CdS band offsets in the literature. However, the band offset varies widely probably because of the difference in the interface structures, in particular, the presence or absence of an interface phase between the CIS and CdS phases. Löher *et al.*[3] reported that the valence band offset with respect to CIS is -0.8 ± 0.1 eV when there is a polycrystalline CdS overlayer on a *p*-CIS (011) substrate. No interphase layer was observed in their room temperature deposition experiment.[3] Nelson *et al.*[9] obtained a CIS/CdS valence band offset of -0.9 ± 0.1 eV; there was no interface layer in their results. Schmit *et al.*[4] showed a net *p*-CIS/CdS band offset of −1.08 eV when there is an ordered defect chalcopyrite (ODC) layer between *p*-CIS and *n*-CdS. The reported *p*-CIS/*n*-ODC and *n*-ODC/*n*-CdS band offsets are −0.28 and −0.8 eV. This *n*-ODC/*n*-CdS offset[4] coincides with Löher *et al.*'s CIS/CdS offset value.[3] An older work by Schmit *et al.*[2] showed a net *p*-CIS/*n*-CdS valence band offset of −1.41 eV when there is an ordered vacancy compound (OVC) layer between *p*-CIS and *n*-CdS, with *p*-CIS/*n*-OVC and *n*-OVC/*n*-CdS band offsets of −0.55 and −0.86 eV, respectively. In short, the CIS/CdS band offset varies widely with the nature of the interface between the two phases. Other CIS/CdS band offsets reported in the literature, where the interface structure is unknown, include −0.6 ± 0.1 eV for ultrahigh vacuum-cleaved CIS/vacuum evaporated CdS[10] and -1.18 ± 0.10 eV for cyanide-treated CIS/CdS.[11] The range of CIS/CdS valence band offsets calculated in this work, which is −1.25 to −0.74 eV, is a good estimate of the experimentally observed values of −1.41 to −0.6 eV.[2–4,9–11]

Schmit *et al.*[2] has also investigated the CIS/OVC/ZnS interface, where the CIS/OVC and OVC/ZnS band offsets are −0.55 and −0.62 eV, respectively, resulting in a net CIS/ZnS offset of −1.17 eV. This is within the range of the CIS/ZnS natural band offset of −1.34 to −0.66 eV (Table V) and the simplified natural band offset of −1.39 to −0.87 eV (Table VI) calculated in this work.

TABLE VII. Natural IP differences obtained from various CIS, CdS, and ZnS surfaces. Values corresponding to the natural interface valence band offsets with respect to CIS are shown in eV.

	CIS/CdS	CIS/ZnS
Nonfaceted	−1.08	−1.23
Faceted	−1.08	−1.22
$(2V_{Cu} + In_{Cu})$	−1.07	−1.22
$(Cu_{In} + In_{Cu})$	−1.45	−1.59

IV. CONCLUSIONS

We have investigated the valence band offset of the faceted and nonfaceted CIS/CdS and CIS/ZnS (110) interfaces using hybrid density functional theory calculations. The excess energies of CIS/CdS and CIS/ZnS interfaces become low when there are no ordered point defects, which is in contrast with the surfaces of CIS that stabilize when such defects form. Both the strained and natural band offsets are relatively independent of the configurations of atoms at the interface, even when there are ordered defects, as long as there are no charged layers. Surface calculations suggest that the reference level, which is given by the average electrostatic potential at the atomic site, is not affected strongly by strain. The simplified natural band offset is defined on the basis of this observation and provides values almost independent of the ILPs used in the interface calculation: −1.23 to −1.18 eV and −1.39 to −1.30 eV for CIS/CdS and CIS/ZnS interfaces, respectively, when there are no Cu vacancies at the interface. The reference level alignment via surface calculations appears to cause slight overcorrections, and the simplified natural band offset is therefore suggested to be more suitable for the prediction of the natural band offset. The IP difference cannot be used as a reasonable approximation of the natural band offset because the discrepancy from the simplified natural band offset can exceed 0.3 eV without any consistent tendency to overestimate or underestimate. This discrepancy partly arises because the IP difference neglects interfacial dipole contributions and inevitably involves surface dipole effects that cannot completely cancel out.

ACKNOWLEDGMENTS

This work was supported by JSPS KAKENHI (Grant-in-Aid for Young Scientists (A), grant number 23686089) and the MEXT Elements Strategy Initiative to Form Core Research Center "Tokodai Institute for Element Strategy (TIES)". Computing resources of ACCMS at Kyoto University were used in this work. The VESTA code[52] was used to draw Fig. 1.

*Corresponding author: yoyo.hinuma@gmail.com
†Corresponding author: oba@cms.mtl.kyoto-u.ac.jp

[1] S. Wagner, J. L. Shay, P. Migliorato, and H. M. Kasper, Appl. Phys. Lett. **25**, 434 (1974).
[2] D. Schmid, M. Ruckh, F. Grunwald, and H. W. Schock, J. Appl. Phys. **73**, 2902 (1993).
[3] T. Löher, W. Jaegermann, and C. Pettenkofer, J. Appl. Phys. **77**, 731 (1995).
[4] D. Schmid, M. Ruckh, and H. W. Schock, Sol. Energy Mater. Sol. Cells **41–42**, 281 (1996).
[5] U. Rau and H. W. Schock, Appl. Phys. A: Materials Science & Processing **69**, 131 (1999).
[6] N. Terada, R. T. Widodo, K. Itoh, S. H. Kong, H. Kashiwabara, T. Okuda, K. Obara, S. Niki, K. Sakurai, A. Yamada, and S. Ishizuka, Thin Solid Films **480–481**, 183 (2005).
[7] R. Herberholz, V. Nadenau, U. Rühle, C. Köble, H. W. Schock, and B. Dimmler, Sol. Energy Mater. Sol. Cells **49**, 227 (1997).
[8] T. Minemoto, Y. Hashimoto, T. Satoh, T. Negami, H. Takakura, and Y. Hamakawa, J. Appl. Phys. **89**, 8327 (2001).
[9] A. J. Nelson, D. W. Niles, C. R. Schwerdtfeger, S. H. Wei, A. Zunger, and H. Höchst, J. Electron Spectrosc. Relat. Phenom. **68**, 185 (1994).
[10] A. Klein, T. Löher, Y. Tomm, C. Pettenkofer, and W. Jaegermann, Appl. Phys. Lett. **70**, 1299 (1997).
[11] Y. Hashimoto, K. Takeuchi, and K. Ito, Appl. Phys. Lett. **67**, 980 (1995).
[12] E. T. Yu, J. O. McCaldin, and T. C. McGill, in *Solid State Physics*, edited by E. Henry and T. David (Academic Press, Boston, 1992), Vol. 46, p. 1.
[13] A. Franciosi and C. G. Van de Walle, Surf. Sci. Rep. **25**, 1 (1996).
[14] A. Walsh and C. R. A. Catlow, J. Mater. Chem. **20**, 10438 (2010).
[15] Y. Hinuma, F. Oba, Y. Kumagai, and I. Tanaka, Phys. Rev. B **86**, 245433 (2012).
[16] C. G. Van de Walle and R. M. Martin, Phys. Rev. Lett. **62**, 2028 (1989).
[17] R. Resta, L. Colombo, and S. Baroni, Phys. Rev. B **41**, 12358 (1990).
[18] A. Franceschetti, S. H. Wei, and A. Zunger, Phys. Rev. B **50**, 17797 (1994).
[19] Y. H. Li, X. G. Gong, and S. H. Wei, Appl. Phys. Lett. **88**, 042104 (2006).
[20] A. Janotti and C. G. Van de Walle, Phys. Rev. B **75**, 121201 (2007).
[21] Y. H. Li, A. Walsh, S. Chen, W. J. Yin, J. H. Yang, J. Li, J. L. F. Da Silva, X. G. Gong, and S. H. Wei, Appl. Phys. Lett. **94**, 212109 (2009).
[22] E. S. Kadantsev and P. Hawrylak, Appl. Phys. Lett. **98**, 023108 (2011).
[23] S. Lany, J. Osorio-Guillén, and A. Zunger, Phys. Rev. B **75**, 241203 (2007).
[24] J. E. Jaffe and A. Zunger, Phys. Rev. B **64**, 241304 (2001).
[25] S. Siebentritt, N. Papathanasiou, J. Albert, and M. C. Lux-Steiner, Appl. Phys. Lett. **88**, 151919 (2006).
[26] A. Seidl, A. Görling, P. Vogl, J. A. Majewski, and M. Levy, Phys. Rev. B **53**, 3764 (1996).
[27] P. E. Blöchl, Phys. Rev. B **50**, 17953 (1994).
[28] J. Heyd, G. Scuseria, and M. Ernzerhof, J. Chem. Phys. **118**, 8207 (2003).
[29] J. Heyd and G. Scuseria, J. Chem. Phys. **120**, 7274 (2004).
[30] A. V. Krukau, O. A. Vydrov, A. F. Izmaylov, and G. E. Scuseria, J. Chem. Phys. **125**, 224106 (2006).
[31] G. Kresse and J. Hafner, Phys. Rev. B **48**, 13115 (1993).
[32] G. Kresse and J. Furthmüller, Phys. Rev. B **54**, 11169 (1996).
[33] G. Kresse and D. Joubert, Phys. Rev. B **59**, 1758 (1999).
[34] J. Paier, M. Marsman, K. Hummer, G. Kresse, I. C. Gerber, and J. G. Angyan, J. Chem. Phys. **124**, 154709 (2006).
[35] D. O. Scanlon and A. Walsh, Appl. Phys. Lett. **100**, 251911 (2012).
[36] F. Oba, M. Choi, A. Togo, and I. Tanaka, Sci. Tech. Adv. Mater. **12**, 034302 (2011).

[37]R. Ishikawa, N. Shibata, F. Oba, T. Taniguchi, S. D. Findlay, I. Tanaka, and Y. Ikuhara, Phys. Rev. Lett. **110**, 065504 (2013).
[38]M. Choi, F. Oba, Y. Kumagai, and I. Tanaka, Adv. Mater. **25**, 86 (2013).
[39]P. Ágoston, K. Albe, R. M. Nieminen, and M. J. Puska, Phys. Rev. Lett. **103**, 245501 (2009).
[40]A. Alkauskas, P. Broqvist, F. Devynck, and A. Pasquarello, Phys. Rev. Lett. **101**, 106802 (2008).
[41]J. Vidal, S. Botti, P. Olsson, J. F. Guillemoles, and L. Reining, Phys. Rev. Lett. **104**, 056401 (2010).
[42]F. Oba, A. Togo, I. Tanaka, J. Paier, and G. Kresse, Phys. Rev. B **77**, 245202 (2008).
[43]A. Janotti, J. B. Varley, P. Rinke, N. Umezawa, G. Kresse, and C. G. Van de Walle, Phys. Rev. B **81**, 085212 (2010).
[44]Y. Kumagai, Y. Soda, F. Oba, A. Seko, and I. Tanaka, Phys. Rev. B **85**, 033203 (2012).
[45]J. P. Perdew, K. Burke, and M. Ernzerhof, Phys. Rev. Lett. **77**, 3865 (1996).
[46]S. L. Dudarev, G. A. Botton, S. Y. Savrasov, C. J. Humphreys, and A. P. Sutton, Phys. Rev. B **57**, 1505 (1998).
[47]J. W. Matthews and A. E. Blakeslee, J. Cryst. Growth **27**, 118 (1974).
[48]L. Kleinman, Phys. Rev. B **24**, 7412 (1981).
[49]C. Rincón, S. M. Wasim, and J. L. Ochoa, Phys. Status Solidi A **148**, 251 (1995).
[50]P. W. Li, R. A. Anderson, and R. H. Plovnick, J. Phys. Chem. Solids **40**, 333 (1979).
[51]S. H. Wei and A. Zunger, J. Appl. Phys. **78**, 3846 (1995).
[52]K. Momma and F. Izumi, J. Appl. Crystallogr. **44**, 1272 (2011).
[53]H. W. Spiess, U. Haeberlen, G. Brandt, A. Räuber, and J. Schneider, Phys. Status Solidi B **62**, 183 (1974).
[54]M. V. Yakushev, F. Luckert, C. Faugeras, A. V. Karotki, A. V. Mudryi, and R. W. Martin, Appl. Phys. Lett. **97**, 152110 (2010).
[55]R. J. Traill and R. W. Boyle, Am. Mineral. **40**, 555 (1955).
[56]S. Adachi, *The Handbook on Optical Constants of Semiconductors: In Tables and Figures* (World Scientific Publishing Company, Singapore, 2012).
[57]G. J. McIntyre, G. Moss, and Z. Barnea, Acta Crystallogr. Sect. A **36**, 482 (1980).